Supplementary information

Remarkable CO_x tolerance of Ni^{3+} active species in Ni_2O_3 catalyst for sustained electrochemical urea oxidation

Muhammed Safeer N. K.,[a,b] Chandraraj Alex, [a] Rajkumar Jana[c], Ayan Datta[c] Neena S John[a]*

[a]Centre for Nano and Soft Matter Sciences, Shivanapura, Bengaluru 562162, India
[b]Manipal Academy of Higher Education, Manipal 576104, India
[c] School of Chemical Sciences, Indian Association for the Cultivation of Science (IACS), Kolkata 700032, India

Corresponding author Email: jsneena@cens.res.in

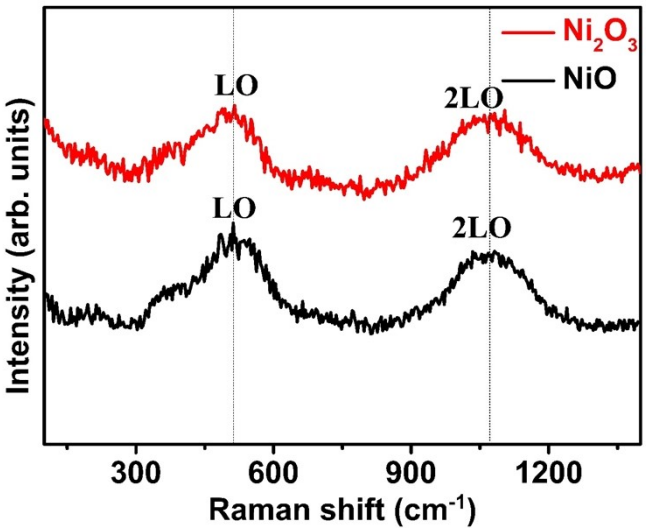

Figure S1. Raman spectra of NiO and Ni_2O_3

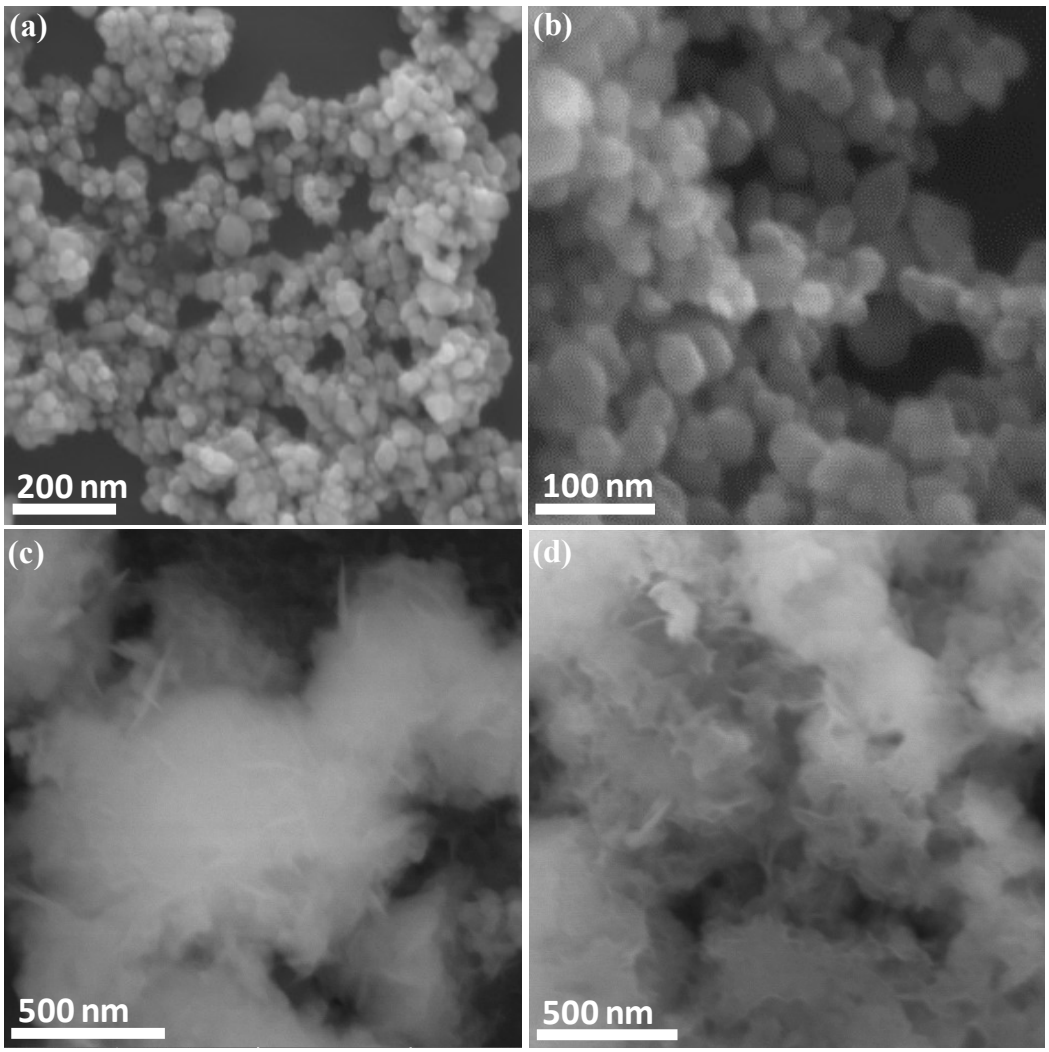

Figure S2. FESEM images of (a, b) NiO and (c, d) Ni_2O_3.

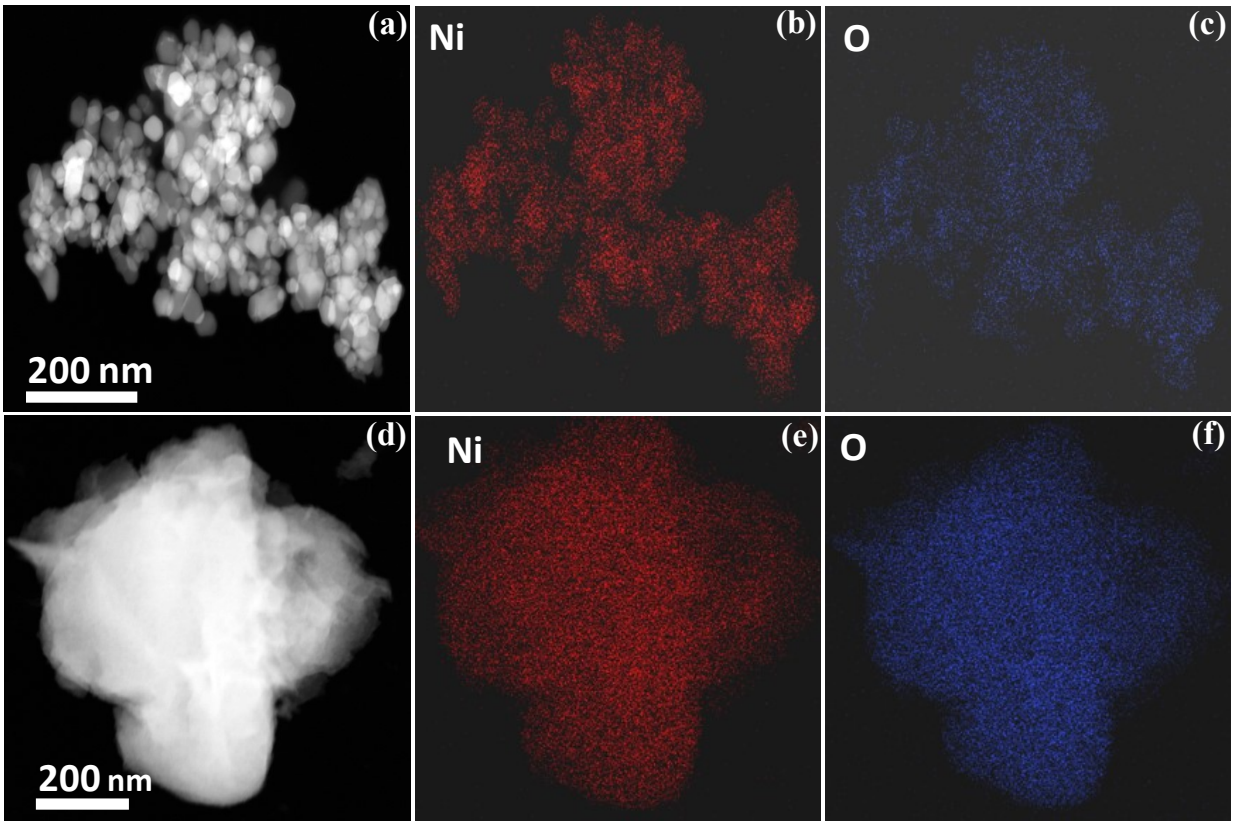

Figure S3. HAADF images and EDS elemental mapping of (a, b and c) NiO and (d, e and f) Ni_2O_3 in STEM mode.

Table S1. Elemental composition of nickel and oxygen in NiO and Ni_2O_3 from TEM

NiO			**Ni_2O_3**		
Element	*Atomic %*	*O/Ni Ratio*	*Element*	*Atomic %*	*O/Ni Ratio*
Nickel	40.33	1.48	Nickel	22.31	3.48
Oxygen	59.66		Oxygen	77.68	

Table S2. Percentage of oxygen from deconvoluting O1s spectra of NiO and Ni_2O_3

Sample	O_1 (%) – lattice oxygen	O_2 (%) – adsorbed oxygen	O_3 (%) – hydroxide
NiO	57.7 %	42.3 %	---------
Ni_2O_3	43.4 %	41.5 %	15.1 %

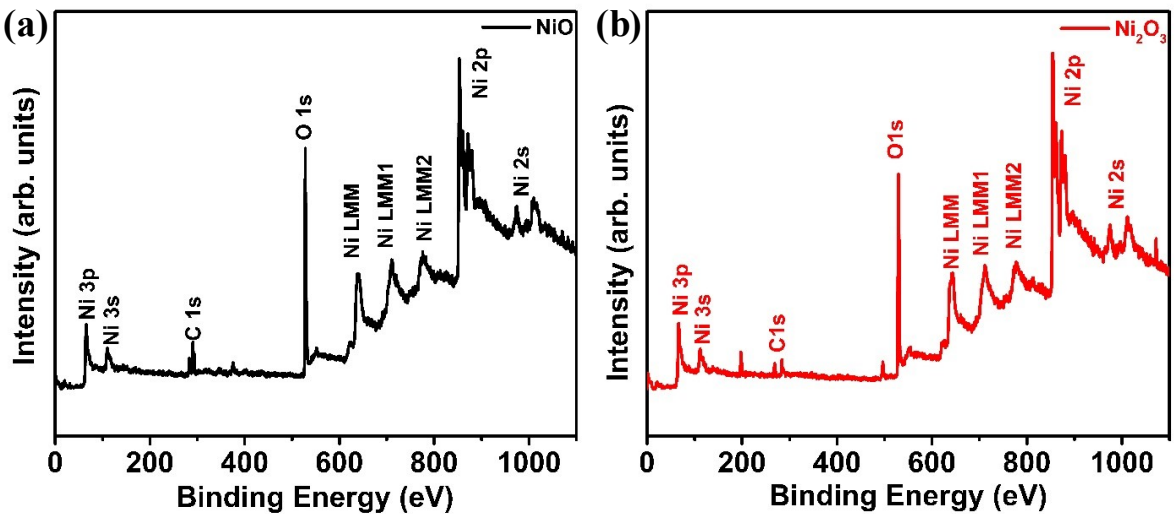

Figure S4. XPS survey spectra of (a) NiO and (b) Ni_2O_3.

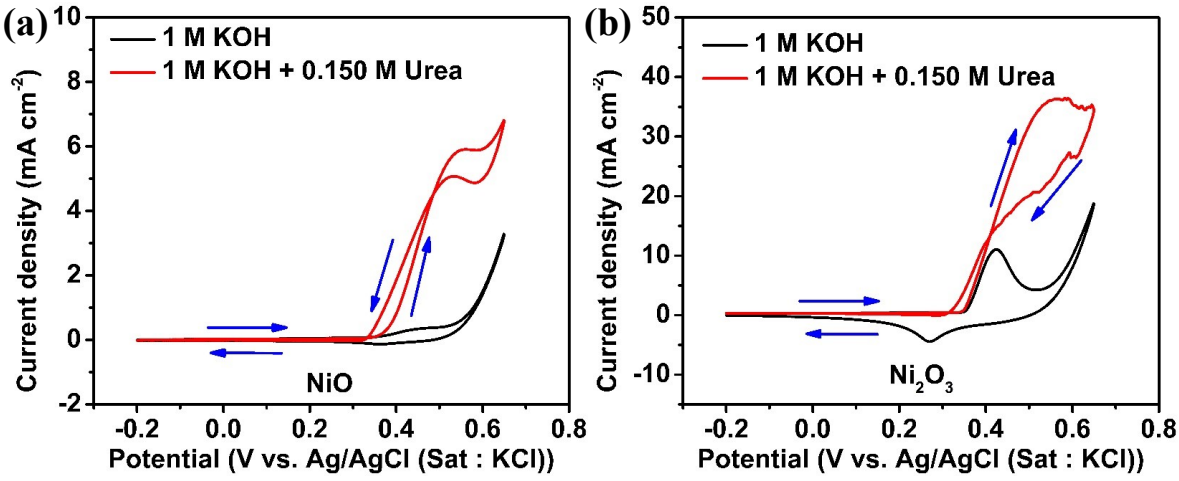

Figure S5. CV of (a) NiO and (b) Ni_2O_3 in 1 M KOH and 1 M KOH + 0.150 M urea at a scan rate of 10 mV s^{-1}

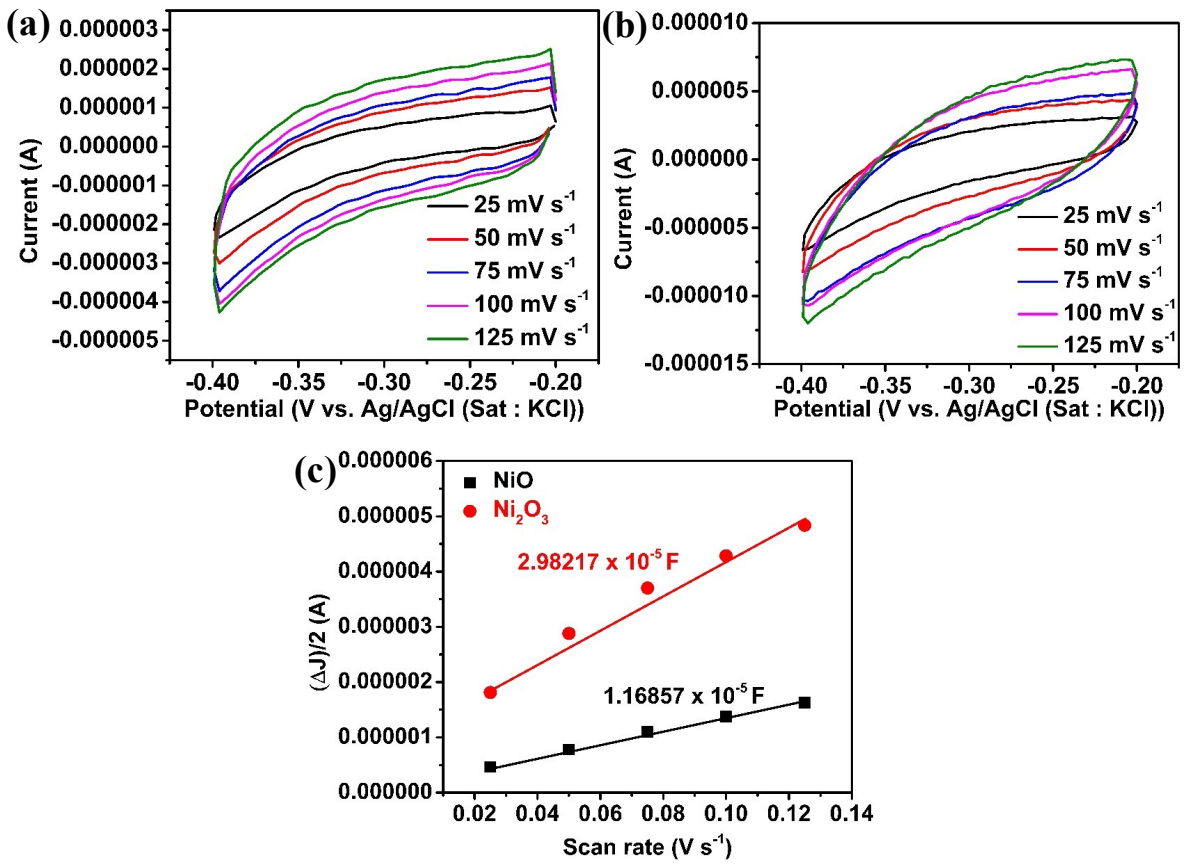

Figure S6. CV of (a) NiO and (b) Ni_2O_3 at various scan rates (25 - 125 mV s^{-1}) in 1 M KOH in the region of −0.4 to −0.2 V vs. $Ag/AgCl_{(sat.KCl)}$ and (c) The capacitive current densities at −0.30 V vs. $Ag/AgCl_{(sat.KCl)}$ as a function of scan rates for NiO and Ni_2O_3

Calculation:

(1) ECSA of NiO : Cdl / Csp = (11.6857 x 10^{-6}) F/ (40 x 10^{-6}) F/cm^{-2} = 0.29 cm^2

(2) ECSA of Ni_2O_3 : Cdl / Csp = (29.8217 x 10^{-6}) F / (40 x 10^{-6}) F/cm^{-2} = 0.74 cm^2

(Csp = average specific capacitance Ni_xO_y systems[1])

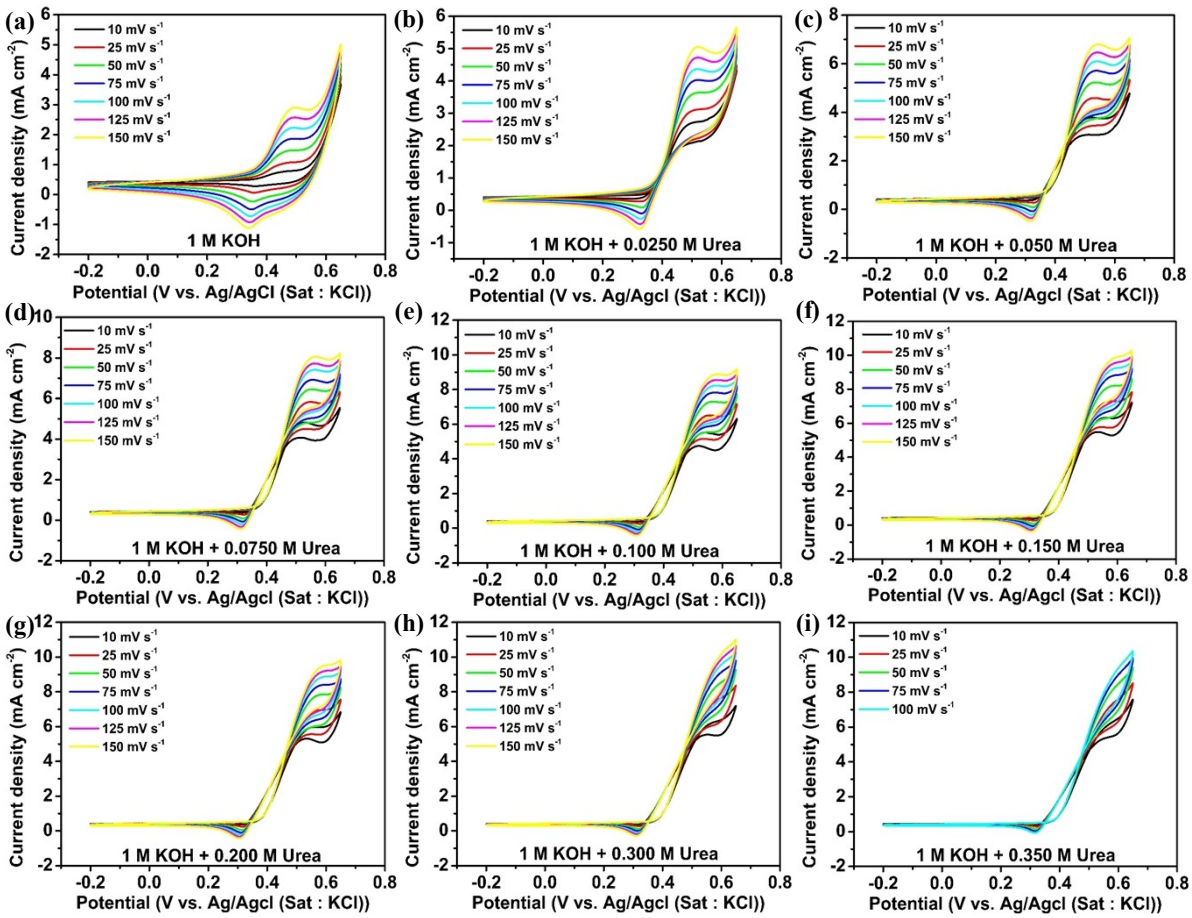

Figure S7. CVs showing UOR activity of NiO catalyst in 1 M KOH containing different urea concentration at various scan rates from 10 - 150 mV s^{-1} (a) 0.000 M urea, (b) 0.025 M urea, (c) 0.050 M urea, (d) 0.075 M urea, (e) 0.100 M urea, (f) 0.150 M urea, (g) 0.200 M urea, (h) 0.300 M urea and (i) 0.350 M urea.

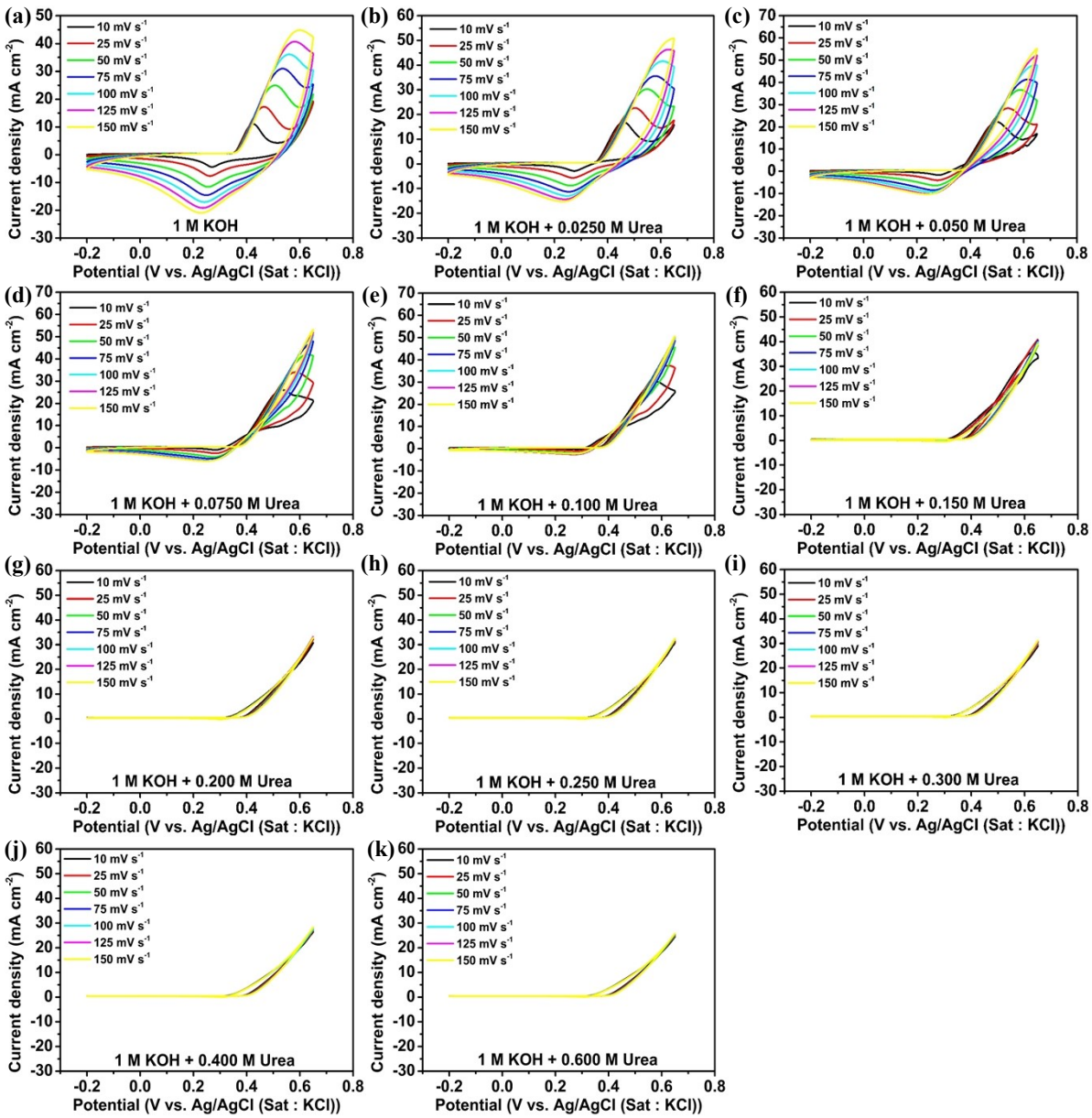

Figure S8. CVs showing UOR activity of Ni_2O_3 catalyst in 1 M KOH containing different urea concentration at various scan rates from 10 - 150 mV s^{-1} (a) 0.000 M urea, (b) 0.025 M urea, (c) 0.050 M urea, (d) 0.075 M urea, (e) 0.100 M urea, (f) 0.150 M urea, (g) 0.200 M urea, (h) 0.250 M urea, (i) 0.300 M urea, (j) 0.400 M urea and (k) 0.600 M urea.

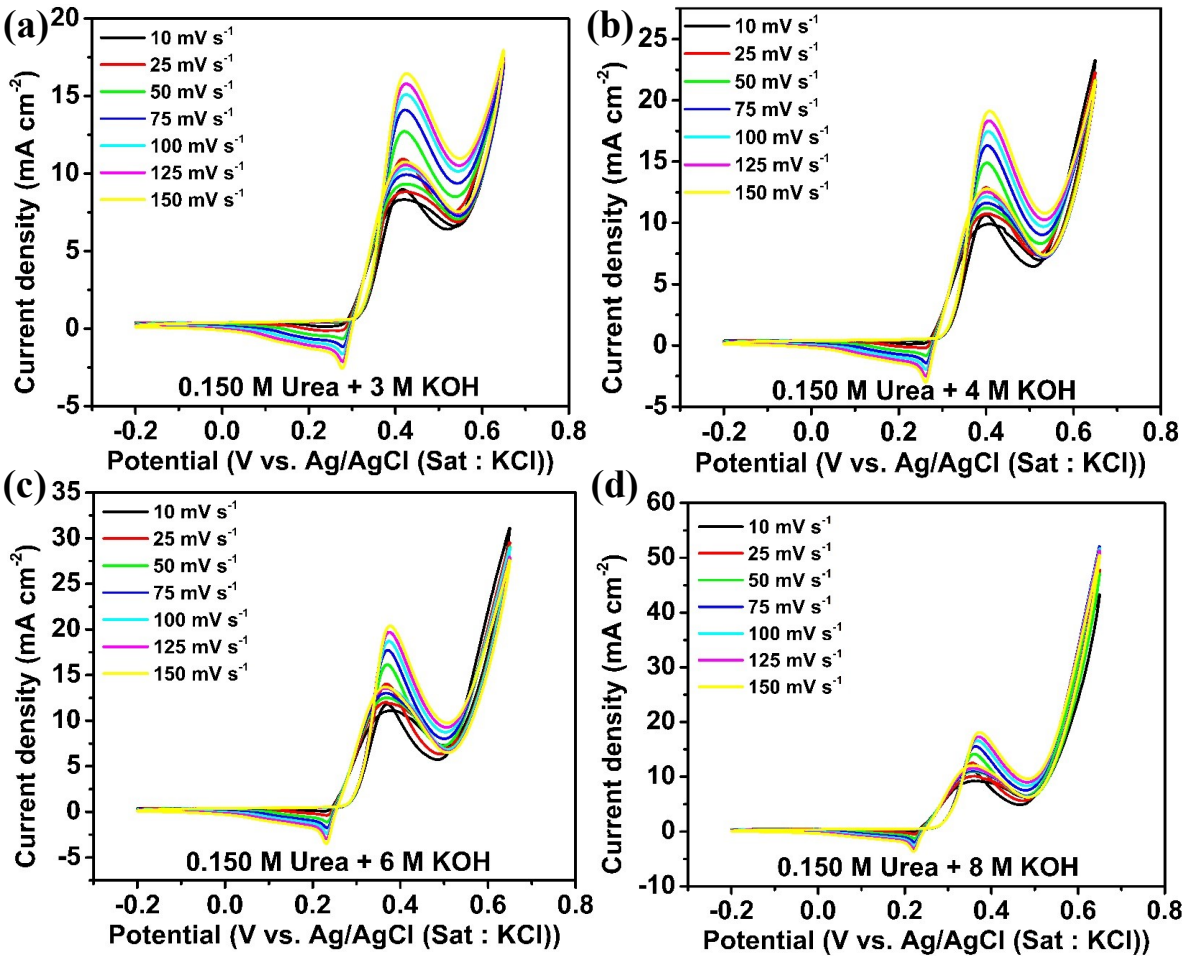

Figure S9. CVs showing UOR activity of NiO catalyst in different molar KOH solution containing 0.150 M urea acquired at various scan rates, 10 - 150 mV s^{-1} (a) 3 M KOH, (b) 4 M KOH, (c) 6 M KOH and (d) 8 M KOH.

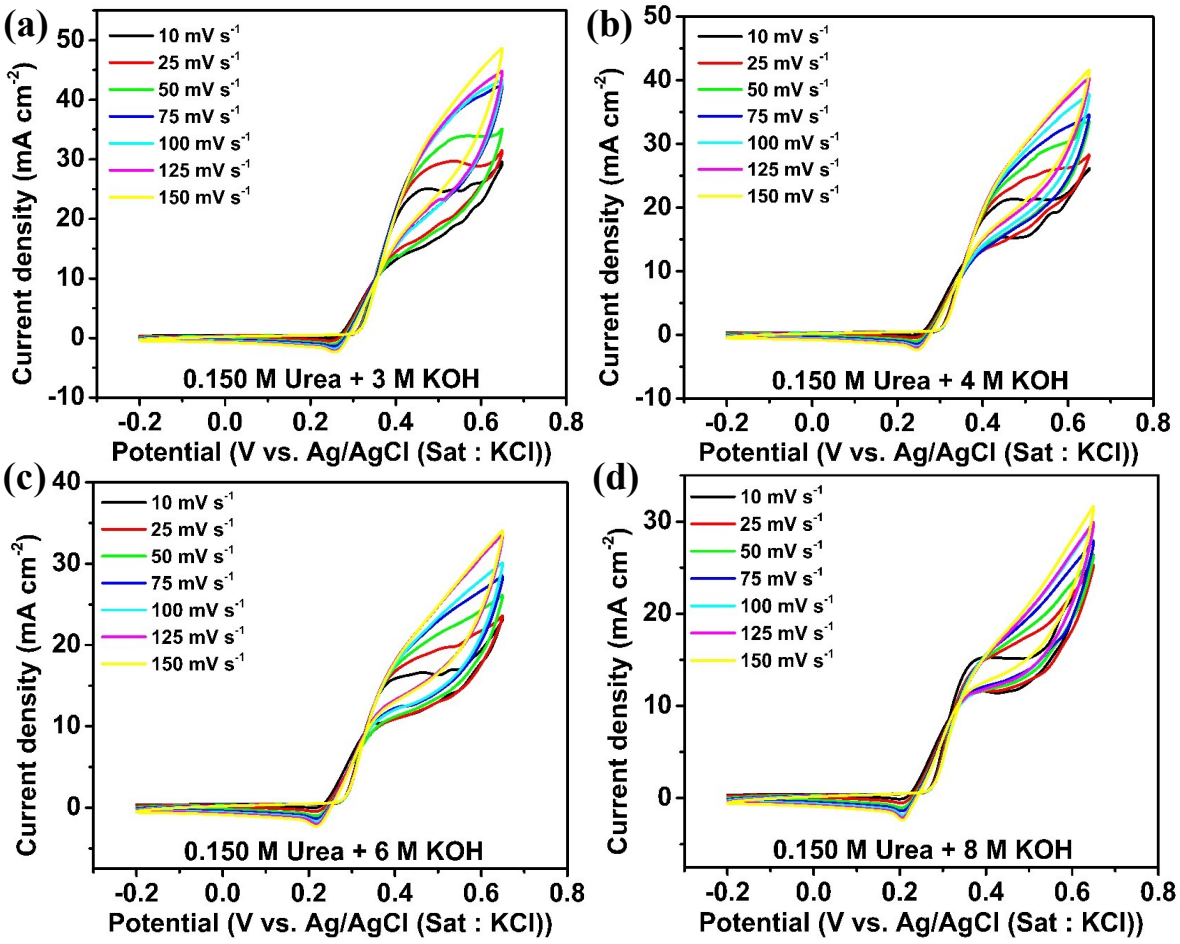

Figure S10. CVs showing UOR activity of Ni_2O_3 catalyst in different molar KOH solution containing 0.150 M urea acquired at various scan rates, 10 - 150 mV s^{-1} (a) 3 M KOH, (b) 4 M KOH, (c) 6 M KOH and (d) 8 M KOH.

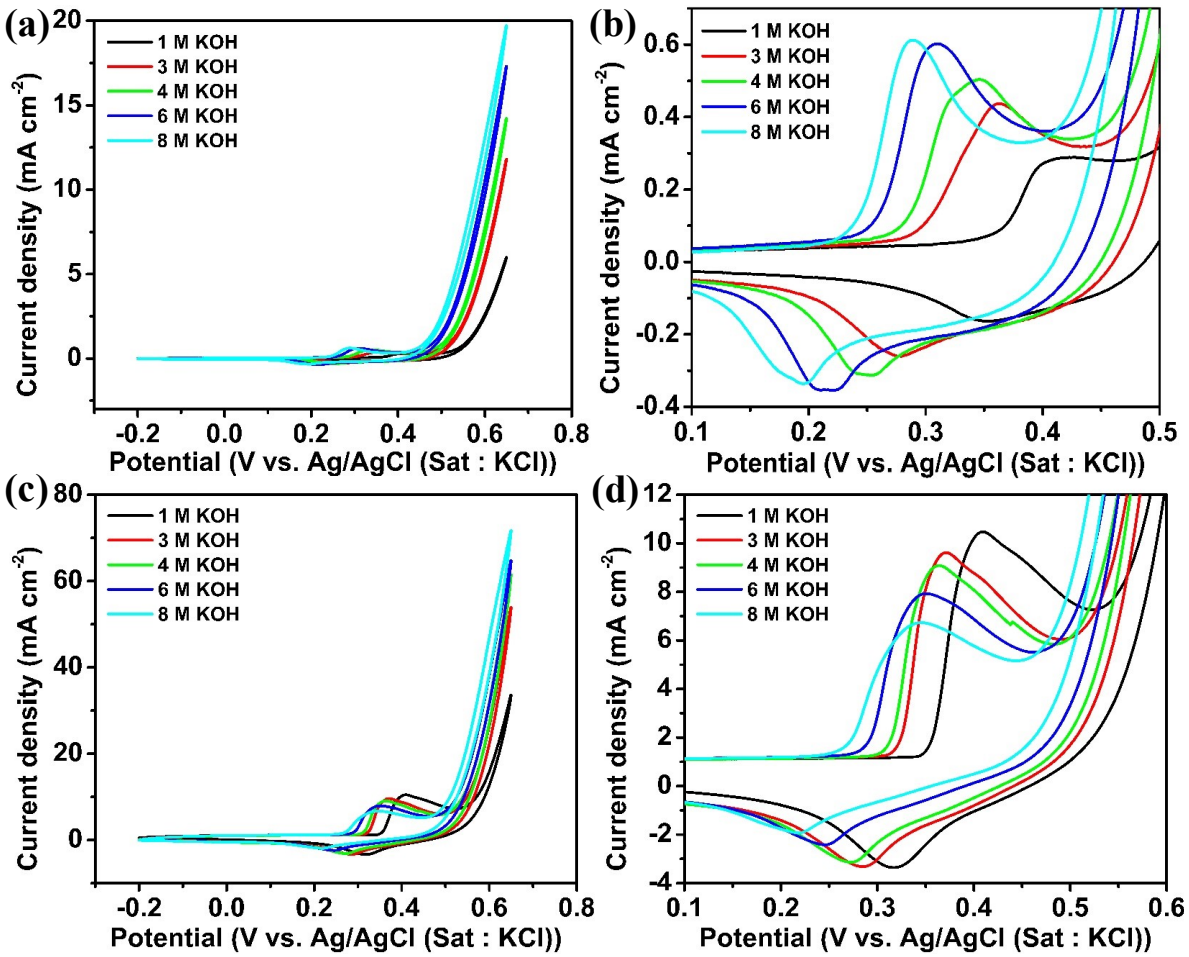

Figure S11. CVs of (a) NiO, (b) magnified view, (c) Ni_2O_3 (d) magnified view, in 1 to 8 M KOH at a scan rate of 10 mV s^{-1}.

Table S3. Applied potential values at which the Z_{real} (real impedance) showing positive and negative values at different concentrations of KOH electrolyte solution containing 0.150 M urea for NiO and Ni_2O_3.

NiO								
1 M KOH +0.150 M Urea			*3 M KOH +0.150 M Urea*			*6 M KOH +0.150 M Urea*		
Positive Z_{real} (Lower potential)	Negative Z_{real} (Mid potential)	Positive Z_{real} (Higher potential)	Positive Z_{real} (Lower potential)	Negative Z_{real} (Mid potential)	Positive Z_{real} (Higher potential)	Positive Z_{real} (Lower potential)	Negative Z_{real} (Mid potential)	Positive Z_{real} (Higher potential)
0.34 V	0.48 V	0.56 V	0.30 V	0.40 V	0.52 V	0.26 V	0.36 V	0.48 V
0.36 V	0.52 V	0.58 V	0.34 V	0.44 V	0.56 V	0.30 V	0.38 V	0.52 V
0.38 V	---------	0.60 V	0.36 V	0.48 V	0.58 V	0.34 V	0.40 V	0.56 V
0.40 V	---------	0.64 V	0.38 V	---------	0.60 V	---------	0.44 V	0.58 V
0.44 V	---------	---------	---------	---------	0.64 V	---------	---------	0.60 V
---------	---------	---------	---------	---------	---------	---------	---------	0.64 V
Ni_2O_3								
1 M KOH +0.150 M Urea			*3 M KOH +0.150 M Urea*			*6 M KOH +0.150 M Urea*		
Positive Z_{real} (Lower potential)	Negative Z_{real} (Mid potential)	Positive Z_{real} (Higher potential)	Positive Z_{real} (Lower potential)	Negative Z_{real} (Mid potential)	Positive Z_{real} (Higher potential)	Positive Z_{real} (Lower potential)	Negative Z_{real} (Mid potential)	Positive Z_{real} (Higher potential)
0.34 V	0.48 V	0.64 V	0.30 V	0.36 V	0.52 V	0.26 V	0.38 V	0.50 V
0.36 V	0.50 V	---------	0.32 V	0.38 V	0.56 V	0.30 V	0.40 V	0.52 V
0.38 V	0.52 V	---------	0.34 V	0.40 V	0.58 V	0.32 V	0.44 V	0.56 V
0.40 V	0.56 V	---------	---------	0.44 V	0.60 V	0.34 V	0.48 V	0.58 V
0.44 V	0.58 V	---------	---------	0.50 V	0.64 V	0.36 V	---------	0.60 V
---------	0.60 V	---------	---------	---------	---------	---------	---------	0.64 V

Table S4. Frequency range at which the −phase angle between (+90° to +180°) and (−90° to −180°) for NiO and Ni_2O_3 in different molar KOH solution containing 0.150 M urea.

NiO					
1 M KOH +0.150 M Urea		*3 M KOH +0.150 M Urea*		*6 M KOH +0.150 M Urea*	
Potential @ - Phase angle between (+90° to +180°) and (-90° to -180)	Frequency Range (Hz) **(No. Of data points)**	Potential @ - Phase angle between (+90° to +180°) and (-90° to -180)	Frequency Range (Hz) **(No. Of data points)**	Potential @ - Phase angle between (+90° to +180°) and (-90° to -180)	Frequency Range (Hz) **(No. Of data points)**
0.48 V	$10^{-0.50} – 10^{-2.0}$ **(18 out of 19)**	0.40 V	$10^{-0.83}$ - $10^{-2.0}$ **(12 out of 15)**	0.36 V	$10^{-0.33}$ - $10^{-2.0}$ **(21 out of 22)**
0.52 V	$10^{0.42}$ - $10^{-2.0}$ **(28 out of 30)**	0.44 V	$10^{0.58}$ - $10^{-2.0}$ **(30 out of 32)**	0.38 V	$10^{0.58}$ - $10^{-2.0}$ **(30 out of 32)**
---	---	0.48 V	$10^{0.75}$ - $10^{-2.0}$ **(32 out of 34)**	0.40 V	$10^{0.67}$ - $10^{-2.0}$ **(32 out of 33)**
---	---	---	---	0.44 V	$10^{0.67}$ - $10^{-2.0}$ **(31 out of 33)**
Ni_2O_3					
1 M KOH +0.150 M Urea		*3 M KOH +0.150 M Urea*		*6 M KOH +0.150 M Urea*	
Potential @ -Phase angle between (+90° to +180°) and (-90° to -180)	Frequency Range (Hz) **(No. Of data points)**	Potential @ - Phase angle between (+90° to +180°) and (-90° to -180)	Frequency Range (Hz) **(No. Of data points)**	Potential @ -Phase angle between (+90° to +180°) and (-90° to -180)	Frequency Range (Hz) **(No. Of data points)**
0.48 V	$10^{-1.5}$ - $10^{-2.0}$ **(6 out of 7)**	0.36 V	$10^{-1.83} – 10^{-2.0}$ **(1 out of 3)**	0.38 V	$10^{-0.25}$ - $10^{-2.0}$ **(20 out of 22)**
0.50 V	$10^{-0.92}$ - $10^{-2.0}$ **(4 out of 14)**	0.40 V	$10^{-1.33}$ - $10^{-2.0}$ **(1 out of 8)**	0.40 V	$10^{0.25}$ - $10^{-2.0}$ **(27 out of 28)**
0.52 V	$10^{-0.92}$ - $10^{-2.0}$ **(5 out of 14)**	0.44 V	$10^{-1.25}$ - $10^{-2.0}$ **(6 out of 10)**	0.44 V	$10^{0.25}$ - $10^{-2.0}$ **(26 out of 28)**
0.56 V	$10^{-1.2}$ - $10^{-2.0}$ **(3 out of 12)**	0.50 V	$10^{-1.67}$ - $10^{-2.0}$ **(1 out of 5)**	0.48 V	$10^{-0.338}$ - $10^{-2.0}$ **(13 out of 21)**
0.58 V	$10^{-0.42}$ - $10^{-2.0}$ **(3 out of 17)**	---	---	---	---
0.60 V	$10^{-0.083}$- $10^{-2.0}$ **(4 out of 24)**	---	---	---	---

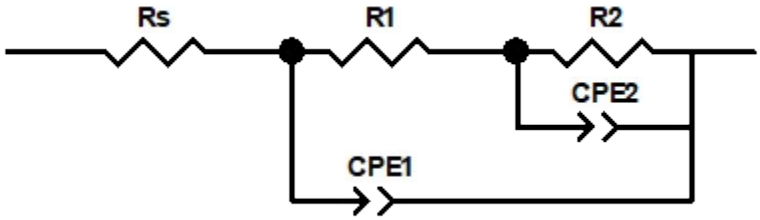

Figure S12. Equivalent circuit for modeling electrochemical urea oxidation on NiO and Ni_2O_3 catalyst

Table S5. Impedance analysis of NiO and Ni_2O_3 in different molar KOH + 0.150 M urea at various potentials. Fitted values based on equivalent circuit given in Fig. S12.

1 M KOH +0.150 M Urea - NiO								
Potential (V)	**Rs**	**R1**	**R2**	**CPE 2-T**	**CPE2-P**	**CPE 1-T**	**CPE1-P**	**X^2**
0.34 V	**16.91**	**1049**	**15862**	**$3.5147x10^{-5}$**	**0.7506**	**$1.1108x10^{-5}$**	**0.89986**	**0.0045955**
0.36 V	**17.01**	**885.4**	**5173**	**$3.5966x10^{-5}$**	**0.75759**	**$1.3828x10^{-5}$**	**0.88649**	**0.0047585**
0.38 V	**17.04**	**602.9**	**2230**	**$4.6456x10^{-5}$**	**0.72061**	**$1.6851x10^{-5}$**	**0.8753**	**0.00054159**
0.40 V	**17.18**	**398.6**	**1456**	**$5.8542x10^{-5}$**	**0.6969**	**$1.9839x10^{-5}$**	**0.86265**	**0.00063567**
0.44 V	**17.66**	**120.6**	**1105**	**0.00010239**	**0.62763**	**$3.0932x10^{-5}$**	**0.83841**	**0.0015716**
0.58 V	**19.64**	**95.17**	**261.7**	**0.00019189**	**0.75729**	**$6.4848x10^{-5}$**	**0.7687**	**0.00033661**
0.60 V	**22.21**	**90.24**	**130**	**0.00030362**	**0.76997**	**$7.5764x10^{-5}$**	**0.75782**	**0.0009636**
0.64 V	**21.65**	**83.86**	**84.18**	**0.00056158**	**0.73407**	**$5.2012x10^{-5}$**	**0.79541**	**0.0014511**
3 M KOH +0.150 M Urea - NiO								
Potential (V)	**Rs**	**R1**	**R2**	**CPE 2-T**	**CPE2-P**	**CPE 1-T**	**CPE1-P**	**X^2**
0.30 V	**6.945**	**469.1**	**4905**	**0.00012759**	**0.631**	**$1.7395x10^{-5}$**	**0.90613**	**0.00072724**
0.34 V	**7.154**	**87.57**	**925.1**	**0.00050303**	**0.43767**	**$2.1847x10^{-5}$**	**0.89958**	**0.00080533**
0.36 V	**7.478**	**103.3**	**772.7**	**0.00054412**	**0.47434**	**$3.3076x10^{-5}$**	**0.86825**	**0.00099556**
0.38 V	**7.689**	**114.2**	**1337**	**0.00063086**	**0.43544**	**$6.6862x10^{-5}$**	**0.8177**	**0.00098234**
0.56 V	**8.692**	**5.662**	**96.22**	**0.00053111**	**0.48474**	**$3.9807x10^{-5}$**	**0.87806**	**0.0011283**
0.58 V	**6.929**	**4.648**	**118.8**	**0.00064334**	**0.42441**	**$3.3455x10^{-5}$**	**0.9104**	**0.0090712**
0.60 V	**8.782**	**15.83**	**210**	**0.0002179**	**0.49499**	**$5.2896x10^{-5}$**	**0.86049**	**0.001484**
6 M KOH +0.150 M Urea - NiO								
Potential (V)	**Rs**	**R1**	**R2**	**CPE 2-T**	**CPE2-P**	**CPE 1-T**	**CPE1-P**	**X^2**
0.26 V	**6.577**	**304.3**	**2995**	**0.00011708**	**0.57674**	**$1.6717x10^{-5}$**	**0.90207**	**0.0016707**
0.30 V	**6.573**	**30.23**	**500.7**	**0.0011774**	**0.29438**	**$2.5277x10^{-5}$**	**0.89934**	**0.00043351**
0.56 V	**8.309**	**14.7**	**48.35**	**0.0010913**	**0.57447**	**$5.3966x10^{-5}$**	**0.86552**	**0.00082237**
0.60 V	**6.827**	**29.7**	**100.1**	**0.00045578**	**0.69883**	**0.00011506**	**0.81544**	**0.001859**
0.64 V	**9.064**	**45.04**	**81.48**	**0.00037345**	**0.77176**	**0.00011919**	**0.79132**	**0.0013519**

1 M KOH +0.150 M Urea - Ni_2O_3								
Potential (V)	**Rs**	**R1**	**R2**	**CPE 2-T**	**CPE2-P**	**CPE 1-T**	**CPE1-P**	**X^2**
0.34 V	**15.71**	**5.171**	**3093**	**$7.6662x10^{-5}$**	**0.69995**	**$1.4029x10^{-5}$**	**0.9**	**0.007714**
0.36 V	**15.12**	**25.45**	**330.7**	**$9.0468x10^{-5}$**	**0.51064**	**0.0001492**	**0.75629**	**0.00044331**
0.38 V	**15.95**	**18.45**	**175.8**	**0.00035398**	**0.42557**	**0.0001845**	**0.73621**	**0.00037078**
0.40 V	**17.44**	**14.23**	**141.7**	**0.001319**	**0.25331**	**0.00027166**	**0.69177**	**0.00047962**
3 M KOH +0.150 M Urea - Ni_2O_3								
Potential (V)	**Rs**	**R1**	**R2**	**CPE 2-T**	**CPE2-P**	**CPE 1-T**	**CPE1-P**	**X^2**
0.30 V	**8.172**	**810.9**	**938.4**	**$6.7161x10^{-6}$**	**0.97826**	**$4.3225x10^{-5}$**	**0.85938**	**0.0023386**
0.32 V	**8.382**	**289.4**	**265**	**0.024806**	**0.2771**	**$9.0863x10^{-5}$**	**0.83638**	**0.00059987**
0.34 V	**8.764**	**146.4**	**167.8**	**0.014057**	**0.36648**	**0.00012378**	**0.81022**	**0.00047635**
0.36 V	**9.086**	**82.8**	**423.7**	**0.0077401**	**0.28471**	**0.00014571**	**0.79912**	**0.00067774**
0.52 V	**9.031**	**62.02**	**116.3**	**0.0028073**	**0.62939**	**0.00014907**	**0.81125**	**0.0015202**
0.64 V	**9.477**	**96.66**	**87.49**	**0.0018702**	**0.63294**	**$8.1524x10^{-5}$**	**0.83062**	**0.0011168**
6 M KOH +0.150 M Urea - Ni_2O_3								
Potential (V)	**Rs**	**R1**	**R2**	**CPE 2-T**	**CPE2-P**	**CPE 1-T**	**CPE1-P**	**X^2**
0.26 V	**6.397**	**1722**	**8568**	**$2.326x10^{-5}$**	**0.67276**	**$2.1197x10^{-5}$**	**0.89634**	**0.0047241**
0.30 V	**6.592**	**149.5**	**404.1**	**0.023626**	**0.23921**	**$9.0437x10^{-5}$**	**0.83869**	**0.00050143**
0.32 V	**6.853**	**98.79**	**373**	**0.012254**	**0.25069**	**0.00012521**	**0.81615**	**0.00143190**

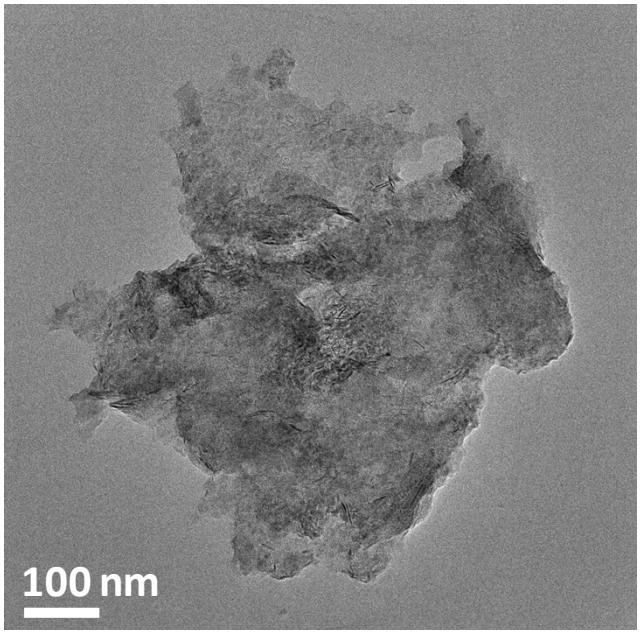

Figure S13. TEM image of Ni_2O_3 after 25 hours of *i-t* measurement

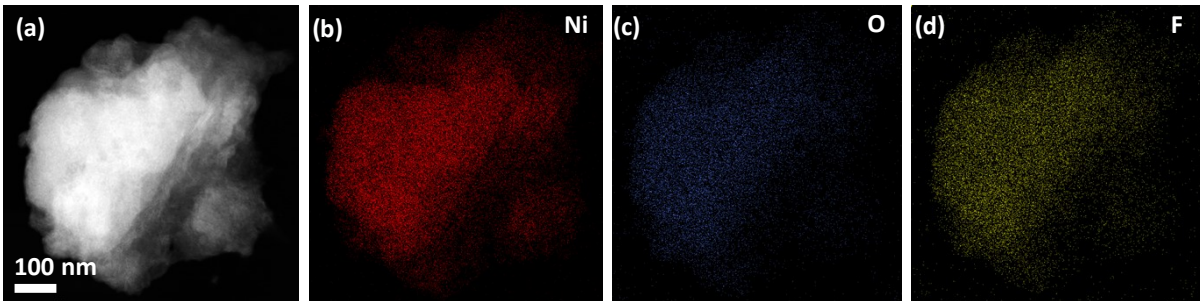

Figure S14. (a) HAADF image of Ni_2O_3 in STEM mode after i-t measurement for 25 hours showing (b) nickel, (c) oxygen from Ni_2O_3 and (d) fluorine from Nafion binder.

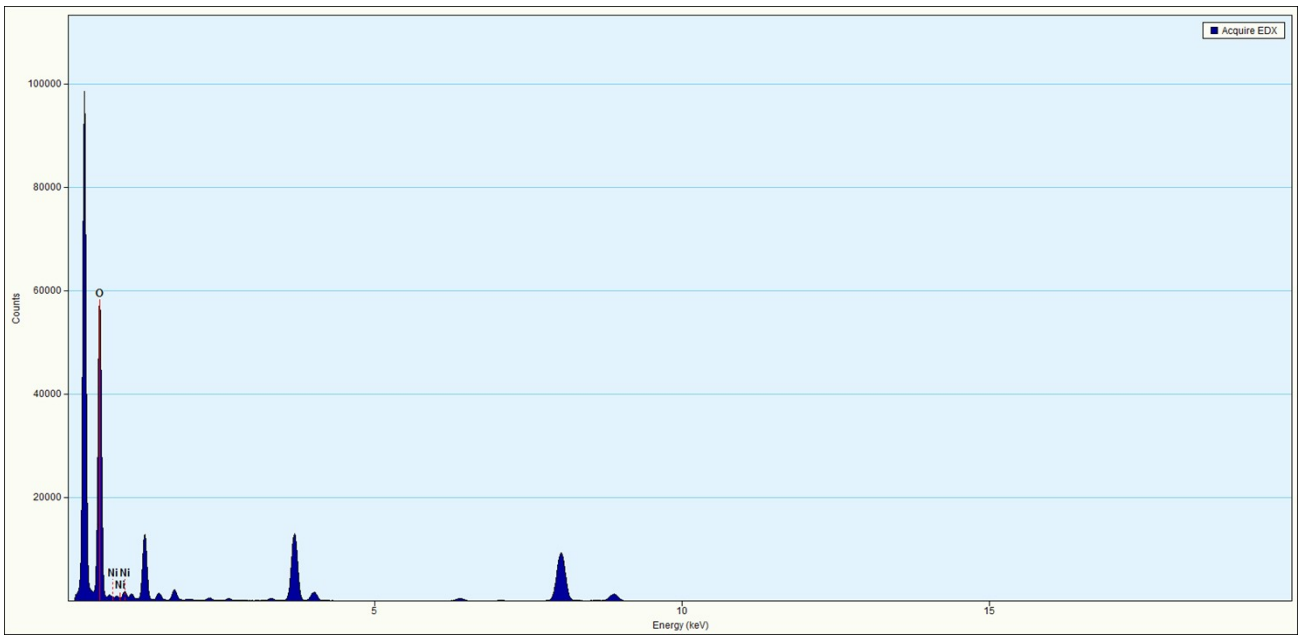

Figure S15. EDS analysis of Ni_2O_3 catalyst after 25 hours of *i-t* measurement.

Computational Details:

All the spin polarized calculations were performed within the framework of density functional theory (DFT) using the plane-wave technique as implemented in Vienna Ab Initio Simulation Package (VASP)[2]. The exchange-correlation energy was accounted within the generalized gradient approximation method (GGA) parameterized by the Perdew-Burke-Ernzerhof (PBE)[3]. The projector augmented wave potential (PAW) was used to treat the ion-electron interactions. The DFT-D2 empirical correction method proposed by Grimme was used for describing the effect of Vander Waals interactions[4]. To account for the on-site

coulomb repulsion, the Hubbard correction parameter U term (DFT+U method) was used to improve the description of localized Ni *d*-electrons in the NiO and Ni_2O_3 surfaces with U_{eff} = 6.45 as recommended by the previous studies[5-6]. In all computations, the kinetic energy cut off is set to be 500 eV in the plane-wave expansion. All the structures were fully relaxed (lattice constant and atomic position) using the conjugated gradient method and the convergence threshold was set to be 10^{-4} eV in energy and 0.01 eV/Å in force. For geometry optimization, the Brillouin zone was sampled using a 3×3×1 Monkhorst-Pack k-point mesh. In order to calculate the charge transfer between different adsorbates and surfaces, we performed Bader charge-population analysis[7-8]. For geometry optimization of the small molecules namely CO_2 and urea ($CO(NH_2)_2$) in gas phase we used B3LYP/6-31+G (d, p) method as implemented in Gaussian 16[9]. The adsorption energies (E_{ad}) of the adsorbates namely OH, CO_2 and $CO(NH_2)_2$ on various surfaces could be defined as

$$E_{ad} = E_{surface+adsorbate} - E_{surface} - E_{adsorbate} \quad (1)$$

where $E_{surface+adsorbate}$ and $E_{surface}$ are the energies of adsorbate adsorbed surfaces and pristine surfaces respectively while $E_{adsorbate}$ is the energy of the adsorbate.[10-11]

According to HRTEM analysis, the surface exposed planes for NiO and Ni_2O_3 surfaces are (111) and (002) respectively. In order to model polar NiO (111) surface, we have considered two type of surface terminations namely Ni-terminated and O-terminated surfaces as suggested by earlier studies.[4,11] The modeled rectangular periodic surface slab (11.55 × 8.87 $Å^2$) of Ni-terminated NiO (111) surface consists of 132 atoms while O-terminated surface slab (12.06 × 8.73 $Å^2$) consists of 154 atoms. On the contrary, Ni_2O_3 (002) surface with one stable Ni-O termination was constructed with a rectangular periodic (3×2) surface slab (13.03 × 9.22 $Å^2$) of 120 atoms. To avoid the spurious interactions between the neighbouring slabs, a vacuum layer of 20 Å was used in the direction perpendicular to the surfaces (along Z-direction) and the nearest distance between the two adsorbed molecules in the adjacent supercell is ~12 Å.

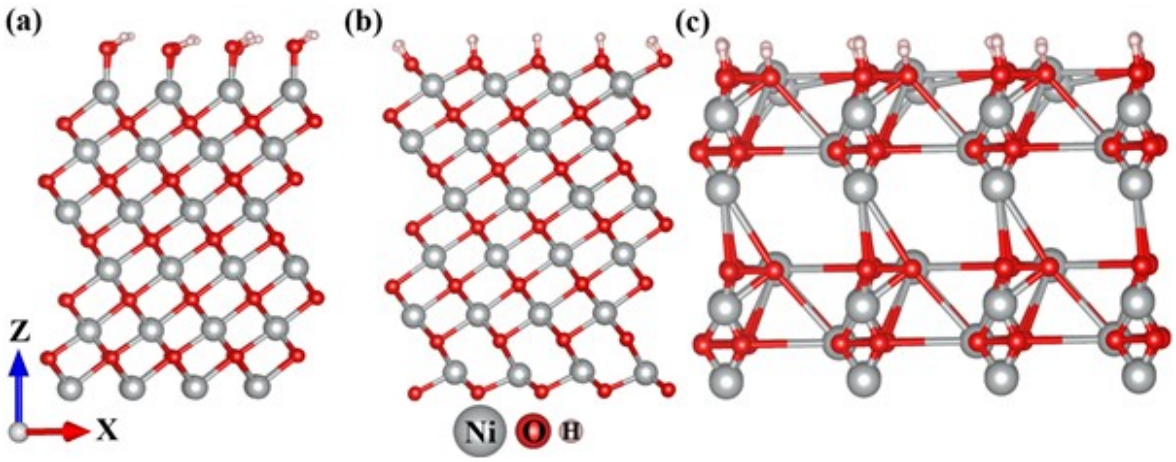

Figure S16. Optimized structures of different in-situ generated hydroxylated surfaces (a) Ni-terminated NiO (111), (b) O-terminated NiO (111), (c) Ni_2O_3 (002).

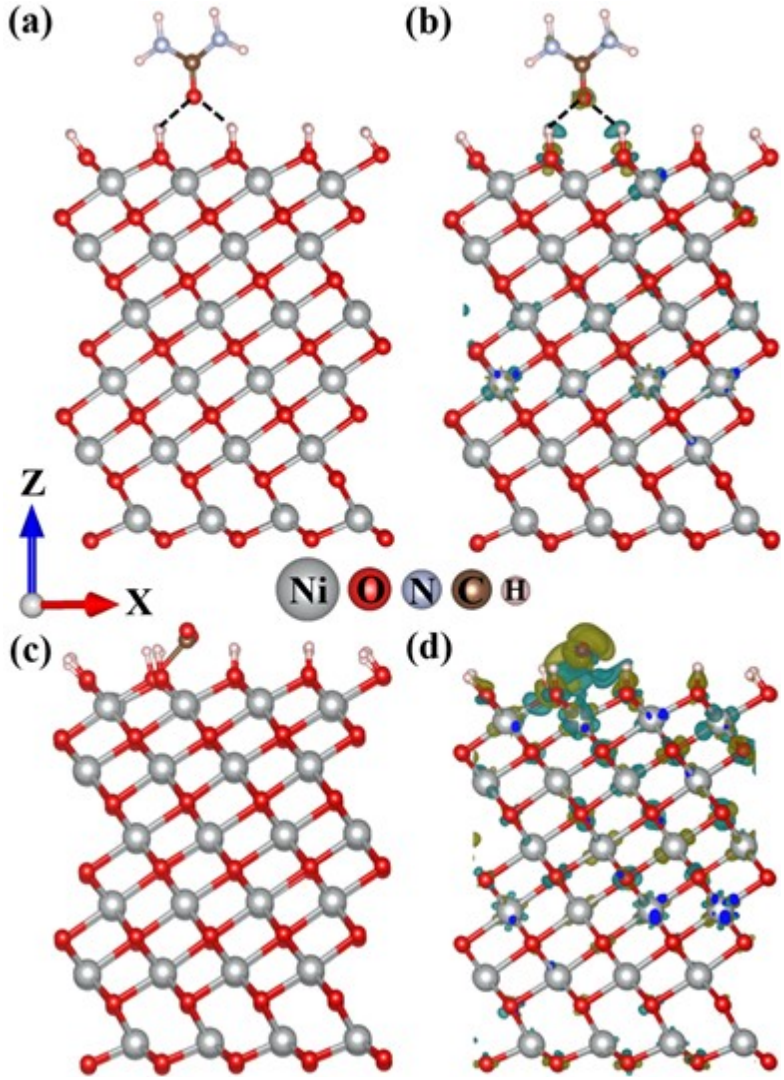

Figure S17. Optimized structures and corresponding charge density difference (CDD) plots of O-terminated NiO (111) surfaces (a-b) urea adsorbed, (c-d) CO_2 adsorbed surfaces. Isodensity value at surfaces is ±0.004 e/a.u.^{3} (positive: cyan and negative: olive) of CDD.

Table S6. Reaction pathway for electrochemical urea oxidation

Steps	Reactions
1	$NiOOH + CO(NH_2)_2 \rightarrow [NiOOH.CO(NH_2)_2]_{ads}$
2	$[NiOOH.CO(NH_2)_2]_{ads} + OH^- \rightarrow [NiOOH.CO(NH_2{\cdot}NH)]_{ads} + H_2O + e^-$
3	$[NiOOH.CO(NH_2{\cdot}NH)]_{ads} + OH^- \rightarrow [NiOOH.CONH_2N]_{ads} + H_2O + e^-$
4	$[NiOOH.CONH_2N]_{ads} + OH^- \rightarrow [NiOOH{\cdot}CONHN]_{ads} + H_2O + e^-$
5	$[NiOOH{\cdot}CONHN]_{ads} + OH^- \rightarrow [NiOOH{\cdot}CO{\cdot}N_2]_{ads} + H_2O + e^-$
6	$[NiOOH{\cdot}CO{\cdot}N_2]_{ads} + OH^- \rightarrow [NiOOH{\cdot}CO{\cdot}OH]_{ads} + N_2 + e^-$
7	$[NiOOH{\cdot}CO{\cdot}OH]_{ads} + OH^- \rightarrow [NiOOH{\cdot}CO_2]_{ads} + H_2O + e^-$
8	$[NiOOH{\cdot}CO_2]_{ads} \rightarrow NiOOH + CO_2$

*Ref[12]

Table S7. Adsorption energies of NiO and Ni_2O_3 catalsyt for OH, urea and CO_2

Sample	OH adsorption energy	Urea adsorption energy	CO_2 adsorption energy
NiO	-0.75 eV	-0.14 eV	-0.98 eV
Ni_2O_3	-0.98 eV	-0.85 eV	-0.45 eV

Table S8. Performance comparison of UOR using Nickel-based catalyst

Sl. No	Catalyst and base electrode	Synthesis method	Electrolyte KOH + Urea	Onset potential	Tafel slope (mV/dec)	Current density (mA cm^{-2})	Stability	Ref
1.	$MnO_2/MnCo_2O_4$ on Nickel foam	Hydrothermal	1 M + 0.5 M	1.33 V vs. RHE	72 mV/dec	10	15 h	**13** *J. Mater. Chem. A*, 2017, **5**, 3208.
2.	Ni_2P NF on Carbon cloth	Hydrothermal	1 M + 0.5 M	0.38 V vs. SCE for 60 mAcm^{-2}	49 mV/dec	Chronopotentiometry at 0.4 V vs. SCE (70mAcm^{-2})	8 h	**14**
3.	Ni-Sn sulfide on	Hydrothermal followed by alkaline	1 M + 0.33 M	1.36 V vs. RHE	32.2	10	12 h	**15**

	Carbon paper	solution etching		for 10 $mAcm^{-2}$	mV/dec			
4.	MoP@NiCo – LDH on Nickel foam	Hydrothermal followed by electrodeposition	1 M + 0.5 M	1.392 V vs. RHE for 100 $mAcm^{-2}$	40 mV/dec	100	20 h	**16** *J. Mater. Chem. A*, 2020, **8**, 18106
5.	Porous $Ni(OH)_2$ nanosheet on GCE	Microwave assisted synthesis	1 M + 0.33 M	1.82 V vs. RHE for 298 $mAcm^{-2}$	43 mV/dec	45	10 h	17
6.	α – $Ni(OH)_2$ nanosheets on Carbon cloth	Hydrothermal	1 M + 0.33 M	-------	-------	300 $mAcm^{-2}$ degraded to 175 $mAcm^{-2}$ in 10 h	10 h	**18**
7.	$LaNiO_3$ on GCE	Reverse phase hydrolysis	5 M + 0.33 M	0.40 V vs. Hg/HgO	-------	600 mAg^{-1} degraded to 150 mAg^{-1} in 1200 seconds	1200 s	**19**
8.	$Ni_{1.5}Mn_{1.5}O_4$ on GCE	Hydrothermal	1 M + 0.33 M	0.29 V vs. Ag/AgCl	--------	20	1000 s	**20**
9.	CNT/C@FeNi on Carbon paper	Pyrolysis	1 M + 60 mM	-------	33 mV/dec	0.85	3 h	**21**
10.	2D MOF – Ni on GCE	Sonication assisted solution method	1 M + 0.33 M	1.36 V vs. RHE for 10 $mAcm^{-2}$	23 mV/dec	20	10 h	22
11.	3D – $Ni_xCo_{2-x}P$ /C@HCN on Carbon cloth	Hydrothermal followed by carbonization and phosphorization	1 M + 0.33 M	1.33 V vs. RHE for 10 $mAcm^{-2}$	74.6 mV/dec	40	6 h	**23**
12.	β – $NiMoO_4$ on Carbon cloth	Hydrothermal	1 M + 0.5 M	1.36 V vs. RHE	48 mV/dec	20	30 h	**24** *ACS Appl. Energy Mater.*, 2020, **3**, 7535
13.	C@NiO on GCE	Hydrothermal followed by pyrolysis	1 M + 0.33 M	1.36 V vs. RHE for 10 $mAcm^{-2}$	87.2 mV/dec	0.015	1800 s	**25**
14.	Ni^0 rich –Ni/NiO Grown on Nickel Foam	Ar/H_2 annealing	1 M + 0.33 M	1350 mV vs. RHE	----------	50	20 h	**26** .*Appl. Surf. Sci.*, 2019, **496**, 143710
15.	Rh-NCs/NiO-NSs on GCE	Mixed cynogels-NaBH4 method	1 M + 0.33 M	1.55 V vs .RHE for 616 mAg^{-1}	36.6 mV/dec	50 mA/g	6000 s	27
16.	Ni-WOx on Nickel foam	Coprecipitation	1 M + 0.33 M	1.40 V vs. RHE for 100 $mAcm^{-2}$	39 mV/dec	100	10 h	28 Angew. Chemie - Int. Ed., 2021, 60, 10577
17.	Mn – Ni3S2 on Nickel foam	Hydrothermal	1 M + 0.5 M	1.303 V vs. RHE for 10 mAcm-2	41.7 mV/dec	50	5.5 h	29
18.	**Ni_2O_3 on GCE**	**Precipitation method**	**1 M + 0.150 M**	**0.340 V vs. Ag/AgCl (1.36 V vs RHE)**	**21 mV/dec**	**25**	**25 h**	**This work**

In the above comparative table, NiO based catalysts with reported stability test ≥ 15 h are highlighted. It can be seen that the UOR performance parameter, Tafel slope, a measure of the kinetics, is the lowest obtained in our case compared to all the reported ones. The urea concentration is also quite low, 0.15 M in the present case. Only one catalyst has reported stability for 30 h but still possesses higher Tafel slope and lower current density than Ni_2O_3. A few catalysts have reported higher current density > 50 mA/cm^2, but it may be noted that such higher current density is observed only for catalysts grown on Ni foam electrodes, which itself contribute to the performance largely.

References

1 C. C. L. McCrory, S. Jung, J. C. Peters and T. F. Jaramillo, *J. Am. Chem. Soc.*, 2013, **135**, 16977–16987.

2 G. Kresse and J. Hafner, *Phys. Rev. B* 1993, **47**, 558.

3 J. P. Perdew, K. Burke, M. Ernzerhof, *Phys. Rev. Lett,* 1996, **77**, 3865

4 S. Grimme, *J. Comput. Chem,* 2006, **27**, 1787-1799.

5 W. Zhao, M . Bajdich, S. Carey, A.Vojvodic, J. K. Nørskov and C.T. Campbell, *ACS Catal*. 2016, **6**, 11, 7377-84.

6 L. Wang, T. Maxisch and G. Ceder, *Phys. Rev. B*, 2006, **73**, 195107.

7 R. F. W. Bader, Atoms in Molecules: A Quantum Theory (Oxford University Press, Oxford,1990).

8 G. Henkelman, A. Arnaldsson and H. Jónsson, *Comput. Mater. Sci*, 2006, **36**, 354–360.

9 M. J. Frisch, et al., Gaussian 16, revision C.01; Gaussian, Inc.: Wallingford, CT, 2016.

10 R. Jana, C. Chowdhury, S. Malik, and A. Datta, *ACS Appl. Energy Mater,* 2019, **2**, 5613−5621.

11 R. Jana, A. Datta and S. Malik, *Chem. Commun*, 2021, **57**, 4508-4511.

12 S. Lu, M. Hummel, S. Kang, R. Pathak, W. He, X. Qi and Z. Gu, *ACS Omega*. 2021, **6**, 22, 14648-14654.

13 C. Xiao, S. Li, X. Zhang and D. R. MacFarlane, *J. Mater. Chem. A*, 2017, **5**, 7825–7832.

14 D. Liu, T. Liu, L. Zhang, F. Qu, G. Du, A. M. Asiri and X. Sun, *J. Mater. Chem. A*, 2017, **5**, 3208–3213.

15 Z. Ji, J. Liu, Y. Deng, S. Zhang, Z. Zhang, P. Du, Y. Zhao and X. Lu, *J. Mater. Chem. A*, 2020, **8**, 14680–14689.

16 T. Wang, H. Wu, C. Feng, L. Zhang and J. Zhang, *J. Mater. Chem. A*, 2020, **8**, 18106–18116.

17 W. Yang, X. Yang, B. Li, J. Lin, H. Gao, C. Hou and X. Luo, *J. Mater. Chem. A*, 2019, **7**, 26364–26370.

18 C. Lin, Z. Gao, F. Zhang, J. Yang, B. Liu and J. Jin, *J. Mater. Chem. A*, 2018, **6**, 13867–13873.

19 R. P. Forslund, J. T. Mefford, W. G. Hardin, C. T. Alexander, K. P. Johnston and K. J. Stevenson, *ACS Catal.*, 2016, **6**, 5044–5051.

20 S. Periyasamy, P. Subramanian, E. Levi, D. Aurbach, A. Gedanken and A. Schechter, *ACS Appl. Mater. Interfaces*, 2016, **8**, 12176–12185.

21 A. Modak, R. Mohan, K. Rajavelu, R. Cahan, T. Bendikov and A. Schechter, *ACS Appl. Mater. Interfaces*, 2021, **13**, 8461–8473.

22 D. Zhu, C. Guo, J. Liu, L. Wang, Y. Du and S. Z. Qiao, *Chem. Commun.*, 2017, **53**, 10906–10909.

23 S. Rezaee and S. Shahrokhian, *Nanoscale*, 2020, **12**, 16123–16135.

24 K. Hu, S. Jeong, G. Elumalai, S. Kukunuri, J. I. Fujita and Y. Ito, *ACS Appl. Energy Mater.*, 2020, **3**, 7535–7542.

25 S. Lu, M. Hummel, Z. Gu, Y. Wang, K. Wang, R. Pathak, Y. Zhou, H. Jia, X. Qi, X. Zhao, B. Bin Xu and X. Liu, *ACS Sustain. Chem. Eng.*, 2021, **9**, 1703–1713.

26 B. Zhang, S. Wang, Z. Ma and Y. Qiu, *Appl. Surf. Sci.*, 2019, **496**, 143710.

27 G. Ma, Q. Xue, J. Zhu, X. Zhang, X. Wang, H. Yao, G. Zhou and Y. Chen, *Appl. Catal. B Environ.*, 2020, **265**, 1–9.

28 L. Wang, Y. Zhu, Y. Wen, S. Li, C. Cui, F. Ni, Y. Liu, H. Lin, Y. Li, H. Peng and B. Zhang, *Angew. Chemie - Int. Ed.*, 2021, **60**, 10577–10582.

29 H. Yang, M. Yuan, Z. Sun, D. Wang, L. Lin, H. Li and G. Sun, *ACS Sustain. Chem. Eng.*, 2020, **8**, 8348–8355.